SLAC-PUB-16127
October 2014

Analysis of Beam Dynamics in a Circular Higgs Factory*

Yunhai Cai
SLAC National Accelerator Laboratory
Stanford University
Menlo Park, CA 94025, USA

Abstract

We design a circular Higgs factory with a center-of-mass energy of 240 GeV residing in a 50-km tunnel. Aside from two strong focusing systems and a low-emittance lattice in arcs that are required to achieve a factory luminosity of $1.0 \times 10^{34}\mathrm{cm}^{-2}\mathrm{s}^{-1}$, a large momentum aperture of 2% is absolutely necessary to mitigate the effect of beamstrahlung and retain an adequate beam lifetime. This turns out to be the most challenging aspect in the design. We comprehensively study the single-particle dynamics and identity many nonlinear aberrations that limit the performance of the optics.

Submitted to The 55th ICFA Advanced Beam Dynamics Workshop on High Luminosity Circular e+e- Colliders - Higgs Factory, October 9-12, Beijing, China

*Work supported by the Department of Energy under Contract No. DE-AC02-76SF00515.

ANALYSIS OF BEAM DYNAMICS IN A CIRCULAR HIGGS FACTORY*

Yunhai Cai†, SLAC National Accelerator Laboratory, Menlo Park, CA 74024, USA

Abstract

We design a circular Higgs factory with a center-of-mass energy of 240 GeV residing in a 50-km tunnel. Aside from two strong focusing systems and a low-emittance lattice in arcs that are required to achieve a factory luminosity of $1.0 \times 10^{34}\mathrm{cm}^{-2}\mathrm{s}^{-1}$, a large momentum aperture of 2% is absolutely necessary to mitigate the effect of beamstrahlung and retain an adequate beam lifetime. This turns out to be the most challenging aspect in the design. We comprehensively study the single-particle dynamics and identity many nonlinear aberrations that limit the performance of the optics.

INTRODUCTION

Since the discovery of the Higgs particle at LHC, the recent results for ATLAS and CMS have shown that the discovered particle resembles the Higgs boson in the standard model of elementary particles. Because of this remarkable discovery, it becomes increasingly important to precisely measure the property of the particle that gives the mass to all and to study the nature of the spontaneous symmetry breaking in the standard model.

The relatively low mass of the Higgs boson provides an opportunity to build an e^+ and e^- collider to efficiently and precisely measure its properties. In the production channel of $e^+e^- \to HZ$, the beam energy required for such a collider is about 120 GeV, which is only 15% higher than the energy reached about two decades ago at LEP2. Can we design and build a circular Higgs factory (CHF) within a decade? What are the major challenges in the design? In this paper, we will address these questions.

LUMINOSITY

In a collider, aside from its energy, its luminosity is the most important design parameter. For Gaussian beams, we can write the bunch luminosity as

$$\mathcal{L}_b = f_0 \frac{N_b^2}{4\pi\sigma_x\sigma_y} R_h, \tag{1}$$

where f_0 is the revolution frequency, N_b the bunch population, $\sigma_{x,y}$ transverse beam sizes, and R_h is a factor of geometrical reduction due to a finite bunch length σ_z and is given by

$$R_h = \sqrt{\frac{2}{\pi}} a e^{a^2} K_0(a^2), \tag{2}$$

$a = \beta_y^*/(\sqrt{2}\sigma_z)$, β_y^* is the vertical beta function at the interaction point (IP), and K_0 the modified Bessel function. In order to avoid R_h becoming too small, we shall require $\sigma_z \approx \beta_y^*$. Obviously, for a number of n_b bunches, the total luminosity is $\mathcal{L} = n_b \mathcal{L}_b$.

In general, the beam sizes in the luminosity formula are not static variables. They are subject to the influence of the electromagnetic interaction during the collision. Typically, for flat beams, the vertical beam size will be blown up by the beam-beam force. To take this effect into account, we introduce the beam-beam parameter as [1]

$$\xi_y = \frac{r_e N_b \beta_y^*}{2\pi\gamma\sigma_y(\sigma_x + \sigma_y)}, \tag{3}$$

where γ is the Lorentz factor and r_e the classical electron radius. Using this formula for ξ_y, we can rewrite the luminosity as [2]

$$\mathcal{L} = \frac{cI\gamma\xi_y}{2r_e^2 I_A \beta_y^*} R_h, \tag{4}$$

where I is the beam current and $I_A = ec/r_e \approx 17045$ A, the Alfven current. Since ξ_y is limited below 0.1 in most colliders, this formula is often used for estimating an upper bound of the luminosity.

Table 1: Main parameters of a circular Higgs factory.

Parameter	LEP2	CHF
Beam energy, E_0 [GeV]	104.5	120.0
Circumference, C [km]	26.7	47.5
Beam current, I [mA]	4	14.4
SR power, P_{SR} [MW]	11	50
Beta function at IP, β_y^* [mm]	50	2
Bunch length, σ_z [mm]	16.1	1.5
Hourglass factor, R_h	0.98	0.76
Beam-beam parameter, ξ_y	0.07	0.07
Luminosity/IR, $\mathcal{L}$ [$10^{34}\mathrm{cm}^{-2}\mathrm{s}^{-1}$]	0.0125	1.01

In Table 1, we tabulated a set of consistent parameters for a CHF. In contrast to the B-factories [3,4], the beam current is severely limited by the power of synchrotron radiation at very high energy. To reach the factory luminosity, we need to have very strong final focusing systems and a very low emittance lattice. This combination makes the design of optics much more difficult compared with that of the B-factories.

SYNCHROTRON RADIATION

When an electron is in circular motion with a bending radius ρ, its energy loss per turn to synchrotron radiation is given by

$$U_0 = \frac{4\pi r_e mc^2\gamma^4}{3\rho}. \tag{5}$$

* Work supported by the Department of Energy under Contract Number: DE-AC02-76SF00515.

† yunhai@slac.stanford.edu

This loss has to be compensated by an RF system. The required RF power per ring is

$$P_{SR} = U_0 I/e. \tag{6}$$

For the beam parameters in Table 1 and $\rho = 5.2$ km, we have $U_0 = 3.6$ GeV, which means that electron loses about 2.5% of its energy every turn. Assuming P_{SR} has to be less than 50 MW, the beam current is limited to 14.4mA in the ring. Applying the expression of P_{SR} to the luminosity formula, we obtain

$$\mathcal{L} = \frac{3c\xi_y \rho P_{SR}}{8\pi r_e^3 \gamma^3 \beta_y^* P_A} R_h, \tag{7}$$

where $P_A = mc^2 I_A/e \approx 8.7$ GW. This scaling property of luminosity in e^+e^- colliders at extremely high energy was first given by Richter [5].

For a CHF with beam energy larger than 120 GeV, its beam current will be severely capped by the electrical power consumed by the RF system and therefore a smaller β_y^* seems the only option to reach the required factory luminosity.

BEAMSTRAHLUNG

Another important aspect of very high energy colliding beams is the emission of photons during collision. In general, this phenomenon is well known and called beamstrahlung. Recently, Telnov found [6] that the most limiting effects to a CHF is an event when a high-energy photon is emitted by an electron in the beamstrahlung process. The electron energy loss can be so large that it falls outside of the momentum aperture η in the colliding ring. For a typical CHF, is was suggested that the following,

$$\frac{N_b}{\sigma_x \sigma_z} < \frac{0.1\eta\alpha}{3\gamma r_e^2}, \tag{8}$$

has to be satisfied to achieve 30 minutes of beam lifetime. Here $\alpha \approx 1/137$ is the fine structure constant. If we introduce aspect ratios of beta functions at the IP and emittances in the ring, namely $\kappa_\beta = \beta_y^*/\beta_x^*$ and $\kappa_e = \epsilon_y/\epsilon_x$, this criteria can be rewritten as

$$\frac{N_b}{\sqrt{\epsilon_x}} < \frac{0.1\eta\alpha\sigma_z}{3\gamma r_e^2}\sqrt{\frac{\beta_y^*}{\kappa_\beta}} \tag{9}$$

.

On the other hand, to achieve the beam-beam parameter ξ_y, we need

$$\frac{N_b}{\epsilon_x} = \frac{2\pi\gamma\xi_y}{r_e}\sqrt{\frac{\kappa_e}{\kappa_\beta}}. \tag{10}$$

Combining this equation with Eq. (9), we have

$$\epsilon_x < \frac{\beta_y^*}{\kappa_e}\left(\frac{0.1\eta\alpha\sigma_z}{6\pi\gamma^2\xi_y r_e}\right)^2. \tag{11}$$

Since the quantities like ξ_y, β_y^*, and σ_z are largely determined by the required luminosity and γ by the particle to be studied, this inequality specifies a low-emittance lattice that is required to achieve 30 minutes of beam lifetime. Normally, the natural emittance scales as γ^2. Here it requires a scaling of γ^{-4}, indicating another difficulty in designing a factory with much higher energy beyond 120 GeV.

Table 2: Additional parameters selected to mitigate the beamstrahlung effects and reach 30 minutes in beamstrahlung beam lifetime.

Parameter	LEP2	CHF
Beam energy, E_0 [GeV]	104.5	120.0
Circumference, C [km]	26.7	47.5
Horizontal emittance, ϵ_x [nm]	48	1.7
Vertical emittance, ϵ_y [nm]	0.25	0.0043
Momentum acceptance, η [%]	1.0	2.0
Momentum compaction, α_p [10^{-5}]	18.5	1.43

As shown in Table 2, we need to design a lattice with much smaller emittance than the one in LEP2 to mitigate the beamstrahlung effect. Typically, a low emittance lattice requires smaller dispersion and stronger focusing. Both will lead to an increase in the strength of the sextupole therefore dramatically reduce the dynamic aperture of the storage ring.

In the choice of the main design parameters, we want a factor of 100 increase in luminosity from LEP2. Because of the limit of the electric power, the increase of luminosity is largely achieved by a combination of very small beta functions at the IP and low emittance lattice. In summary, the lattice of a CHF has following main challenges:

- Low emittance lattice at high energy
- High packing factor of magnets
- Strong final focusing
- Large momentum acceptance
- Short bunches

A high packing factor is required to reduce synchrotron radiation in the bending magnets and not increase the circumference of the ring. We will proceed to a specific design to assess how difficult it is to meet these challenges.

ARC

For an electron ring, the horizontal emittnace is given by

$$\epsilon_x = F\frac{C_q\gamma^2}{J_{xd}}\theta^3, \tag{12}$$

where C_q is a constant,

$$C_q = \frac{55}{32\sqrt{3}}\frac{\hbar}{mc}, \tag{13}$$

and θ is the bending angle of the dipole. Here J_{xd} is the damping partition number and typically equals one. F is a factor that depends on the type of cell. For FODO cells, it

is at an order of one. In general, the stronger focusing of a cell, the smaller its F. Clearly, as seen in Eq. (12), the most effective way to reduce the emittance is to make the bending angle in a cell small. That implies that we use more cells.

In the arcs, we choose FODO cells because of their high packing factor and use many cells to reach the required emittance. the 60^0 phase advance is selected due to its property of resonance cancellation that we will explain later. The optics of the cell is illustrated in Fig. 1. Every six cells makes a unit transformation of betatron oscillation. In our design, each arc consists of 32 units and ends with dispersion suppressors. Similar to LEP2, we have eight arcs and eight straight sections to complete a ring with parameters shown in Table 2.

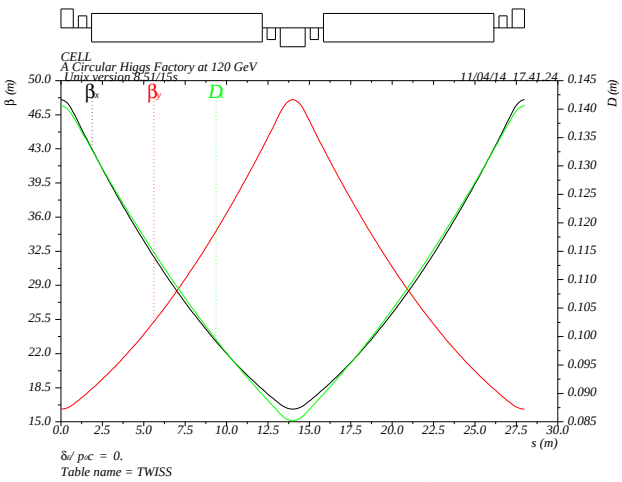

Figure 1: *Lattice functions in a* 60^0 *FODO cell.*

Table 3: The nonlinear chromaticities and tune shifts due to betatron amplitudes in the lattice that consists of arcs and simple straight sections.

Derivatives of tunes	Values
$\partial\nu_{x,y}/\partial\delta$	$0, 0$
$\partial^2\nu_{x,y}/\partial\delta^2$	$-102, +128$
$\partial^3\nu_{x,y}/\partial\delta^3$	$+666, +557$
$\partial\nu_x/\partial J_x\ [m^{-1}]$	-3.08×10^5
$\partial\nu_{x,y}/\partial J_{y,x}\ [m^{-1}]$	-1.02×10^6
$\partial\nu_y/\partial J_y\ [m^{-1}]$	-2.70×10^5

In this study, we set two families of sextupoles to make the linear chromaticity zero in the ring. For the third-order resonances, the contribution of sextupoles to all driving terms along the storage ring are computed [7] using the Lie method and plotted in Fig. 2. As one can see from the figure, they are all canceled out within one betatron unit (made with six cells), as predicted by theorem [8].

For the fourth-order resonances, we find similar cancelations [7] as shown in Fig. 3 except for one resonance:

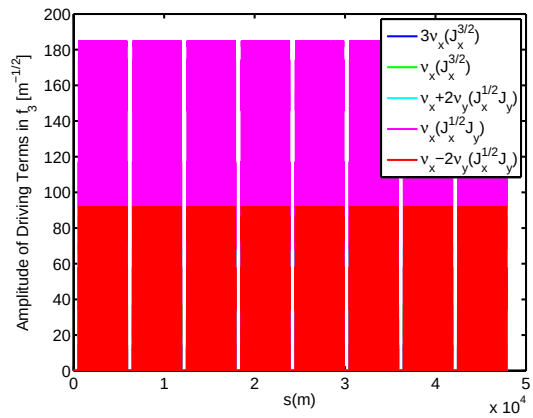

Figure 2: *All third-order resonances driven by sextupoles.*

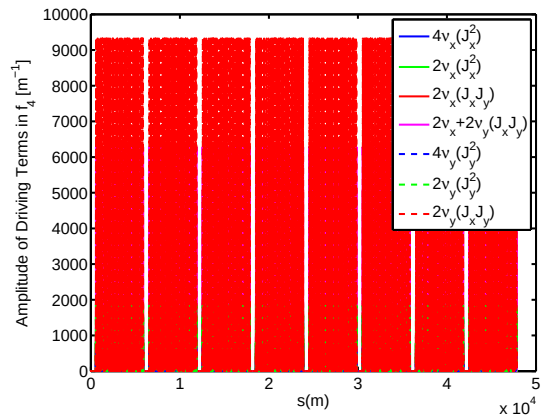

Figure 3: *Fourth-order resonances driven by sextupoles.*

$2\nu_x - 2\nu_y = 0$. Since this resonance overlaps the same the line as the linear coupling resonance in the betatron tune space, we can ignore it because the ring cannot operate near the linear resonance anyway.

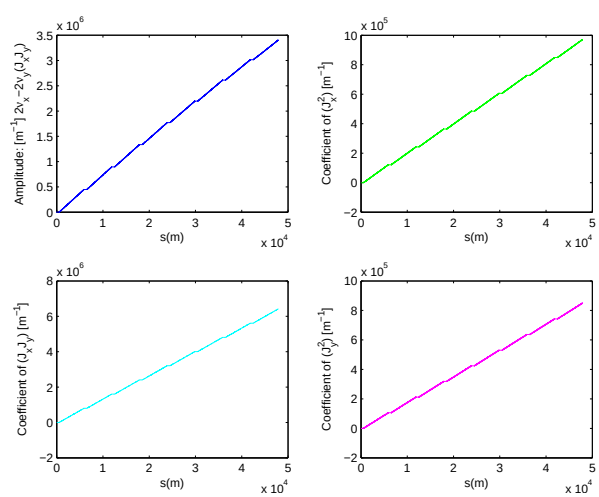

Figure 4: *The four residual 4th-order terms in the Lie operator:* f_4.

It is also worth noting that there are three more terms of geometric aberrations in f_4. They do not drive any resonances but shifts of betatron tunes. All four residual geometric terms in f_4 are shown in Fig. 4 as they are accumulated along in the ring. As we can see, they are continually increasing and reach very large values. To quantify their effects on the beam, we compute the tune shifts along with the high-order chromaticities using the normal form analysis [9] and tabulate the result in Table 3. Comparing with the existing storage rings, these tune shifts are too large at least by an order of two in magnitude.

FINAL FOCUSING SYSTEM

Note that the beam lifetime condition in Eq. (11) does not depend on κ_β. Therefore, according to Eq. (10), κ_β (or β_x^*) can be used to adjust the bunch population N_b or equivalently the number of bunches n_b when the total current is limited by the electrical power. Here we would like to choose a large β_x^*, leading to a smaller n_b. Our choice of the parameters in the interaction region are tabulated in Table 4.

Table 4: Other parameters determined by a specific design of final focusing system.

Parameter	LEP2	CHF
Beam energy, E_0 [GeV]	104.5	120.0
Circumference, C [km]	26.7	47.5
β_x^* [mm]	1500	200
β_y^* [mm]	50	2
Bunch population, N_b [10^{10}]	57.5	32.0
Number of bunches, n_b	4	25

It is always challenging to design a final focusing system (FFS) in a circular collider. In the CHF, it becomes even more so because of a smaller β_y^* (2 mm) and a longer distance L^* (2 meter) which is the distance between the IP and the first focusing quadrupole.

Here we adopt an optics similar to the design of a linear collider. The optics of the FFS is shown in Fig. 5. The FFS starts with a final transformer (FT), continues with a chromatic correction in the vertical (CCY) and then the horizontal plane (CCX), and ends with a matching section. The entire FFS has three imaging points and fits in a 175-meter long straight section.

The FT contains only two quadrupoles which serve as the final focusing doublet. The betatron phase advances are nearly 180^0 in both planes. At the end of the FT, we have the first imaging point where the beta functions remain very small. In our study, we have reduced the number of quadrupoles in this section to maximize the momentum aperture in the FFS. A drawback of this approach is that the beta functions at the end of the FT cannot be adjusted.

The CCY consists of four 90^0 FODO cells and make a unit of betatron transformer. The module starts at the middle of the defocusing quadrupole to enhance the peak of the vertical beta function at the positions of a pair of sextupoles separated by "-I" transformation. Two pairs of dipoles create two dispersion bumps, providing the dispersions at the location of the sextupole. At the end of the CCY, we have the second imaging point at which the lattice functions are identical to those at the first one.

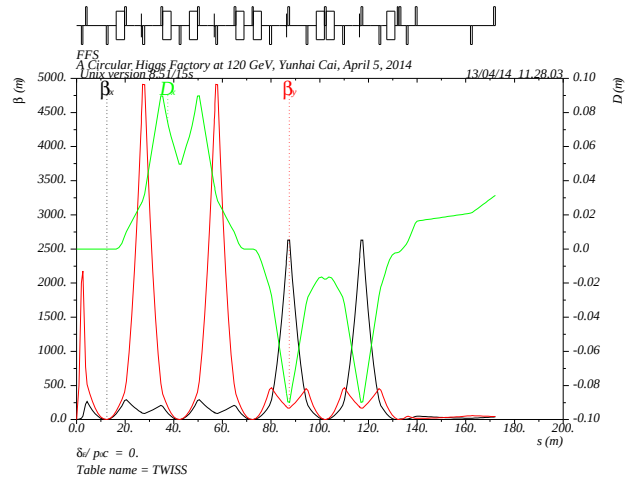

Figure 5: *Lattice functions in a final focusing system with local chromatic compensation section.*

Similarly, we construct the CCX, but starting at the middle of the focusing quadrupole. And at the end of the CCX, we have the third image point. Here, we have essentially compensated the local chromaticity as shown in Fig. 6 and transport the very small beta functions at the IP to the end of the CCX. In the matching module, we can place the quadrupoles near the third imaging point without the worry of L^* and match easily the FFS to the dispersion suppressor.

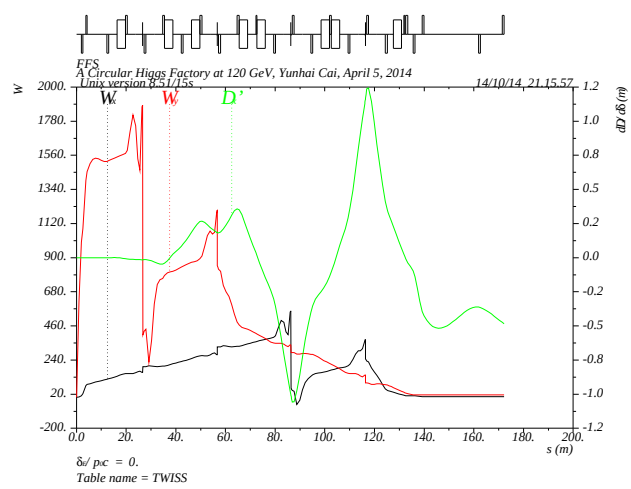

Figure 6: *W function in the final focusing system with the local chromatic compensation.*

Finally, we use the longitudinal cyclical symmetry in the CCY and CCX to adjust the betatron phase between the final

doublet and the sextupole pairs to optimize the second order chromaticity in the FFS. We should note that the second order dispersion leaks out of the FFS as shown in Fig. 6.

Aside from those chromatic aberrations, there are many large geometric and chromatic aberrations in the FFS. As shown in Fig. 7, a fifth-order aberration, $p_x p_y^2 \delta^2$, increases in large steps at the position of the sextupoles in the FFS. It was pointed out by Oide [10] that this aberration can be compensated by a proper setting of asymmetric dispersions at the positions of the pair of sextupoles.

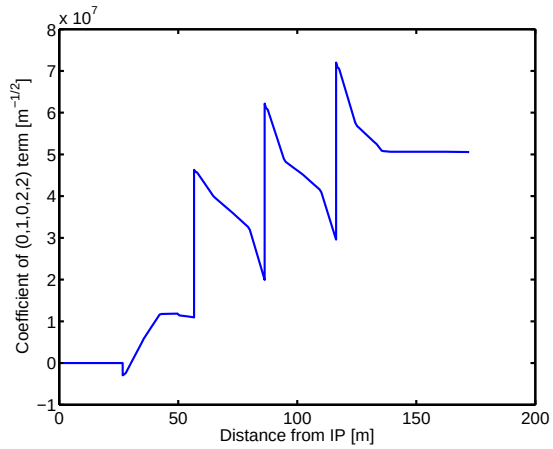

Figure 7: *A fifth order aberration in the single-Lie operator in the normalized coordinates.*

From the analysis, we find also that the largest aberration in fifth-order is $p_y^4 \delta$ as shown in Fig. 8. The source of this aberration is the kinematic term but enhanced by the strong sextupoles. This huge aberration may well be the bottleneck of the FFS. It can significantly degrade the off-momentum aperture of the collider.

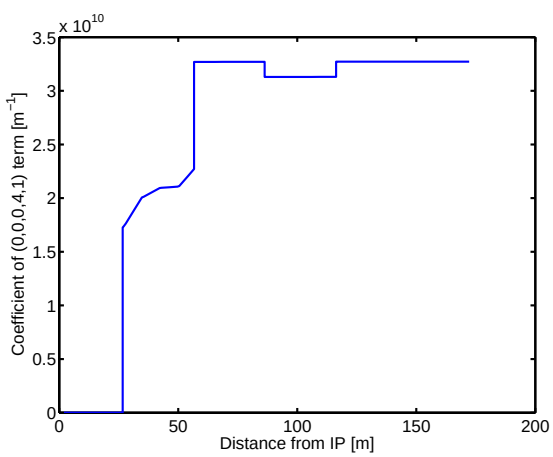

Figure 8: *The largest fifth order aberration in the single-Lie operator in the normalized coordinates.*

COLLIDER

Replacing two interaction regions with two simple straights in the arc lattice, we build a collider lattice shown in Fig. 9.

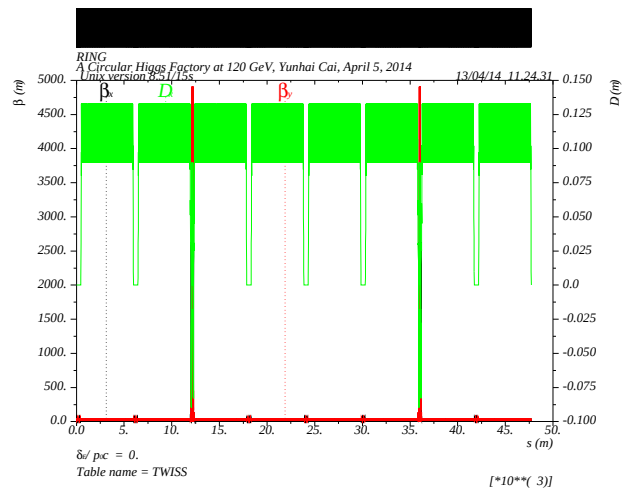

Figure 9: *Lattice functions in the CHF that includes two interaction regions.*

We readjust the settings of two families of the sextupoles in the arcs for a few units of positive chromaticity and obtain the bandwidth of momentum deviation of ±2% as shown in Fig. 10.

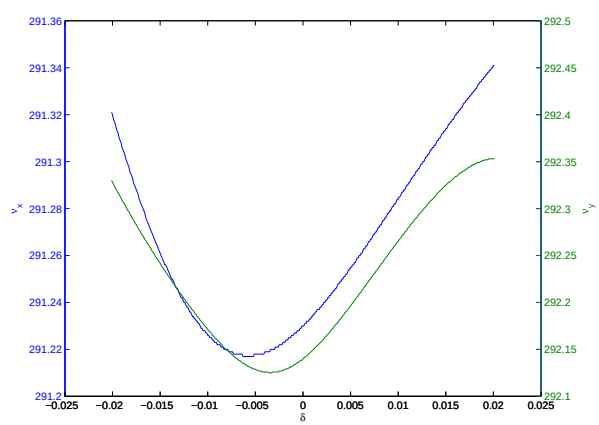

Figure 10: *Betatron tunes of the collider ring as a function of relative momentum.*

Since the strongest quadrupoles and sextupoles are positioned at the highest beta functions in the FFS, naturally the IR contains many high-order aberrations. We compute the third-order and fourth-order driving terms in the collider. The cancellation of the resonances at third-order remains intact. But the fourth-order resonance driving terms become much larger as shown in Fig. 11. Clearly, the aberrations in the IR are dominant in the entire ring. The source of

the fourth-order aberration are the kinematic terms from the perturbation expansion of the Hamiltonian.

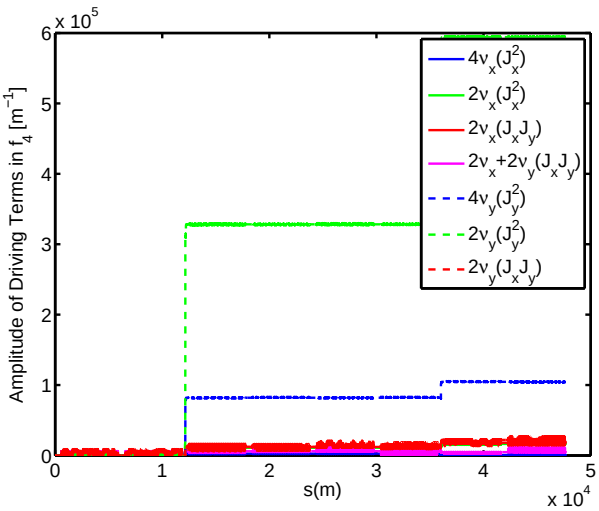

Figure 11: *Fourth-order resonances driving terms in the lattice with two interaction regions.*

To confirm their effects in the collider, we compute the tune shifts, the high-order chromaticities, and geometric and chromatic tune shifts using the normal form analysis and tabulate the result in Table 5. Indeed, the table shows that the geometric and chromatic tune shifts are much larger at $\delta = 0.01$ than the geometric tune shifts, which themselves are already two order of magnitudes too large as mentioned previously.

Table 5: The nonlinear chromaticities and tune shifts due to betatron amplitudes in the collider that contains two interaction regions.

Derivatives of tunes	Values
$\partial\nu_{x,y}/\partial\delta$	$0, 0$
$\partial^2\nu_{x,y}/\partial\delta^2$	$+496, +1750$
$\partial^3\nu_{x,y}/\partial\delta^3$	$-74400, -345000$
$\partial\nu_x/\partial J_x\ [m^{-1}]$	-2.94×10^5
$\partial\nu_{x,y}/\partial J_{y,x}\ [m^{-1}]$	-9.91×10^5
$\partial\nu_y/\partial J_y\ [m^{-1}]$	-1.07×10^5
$\partial^2\nu_x/\partial\delta\partial J_x\ [m^{-1}]$	-1.11×10^9
$\partial^2\nu_{x,y}/\partial\delta\partial J_{y,x}\ [m^{-1}]$	-1.75×10^9
$\partial^2\nu_y/\partial\delta\partial J_y\ [m^{-1}]$	-1.56×10^{10}

CONCLUSION

Despite much progress being made since the last Higgs workshop two years ago, we have not yet solved the problem of the off-momentum dynamic aperture in the collider. From our systematic analysis, we find the following design issues:

- Tune shifts vs. amplitudes are very large due to interlaced sextupoles in the arcs
- The second-order dispersion in the interaction region leads out to the arcs
- Second- and third- order chromaticity are too large in the collider
- Huge geometric-chromatic aberration seen in 5th-order Lie operators in the final focusing system

As shown in our study, the CHF requires not only a final focusing system with an ultra-low beta at the interaction point but also a very low-emittance lattice at very high energy. Such optics in a storage ring with a larger momentum aperture will be the ultimate challenge for our accelerator community in the next decade.

ACKNOWLEDGMENT

I would like to thank Alex Chao, Yuri Nosochkov, Richard Talman, Uli Wienands, and Frank Zimmermann for many stimulating discussions.

REFERENCES

[1] F. Amman and D. Ritson, “Design of electron-positron colliding beam rings," 1961 Inernat. Conf. on High Energy Accelerators, Brookhaven, p471, (1961).

[2] J.T. Seeman, “Beam-beam interaction: luminosity, tails and noise," SLAC-PUB-3182, July (1983).

[3] “PEP-II: An Asymmetric B Factory”, Conceptual Design Report, SLAC-418, June 1993.

[4] “KEKB B-factory Design Report", KEK-Report-95-7, (1995).

[5] B. Richter, “Very high electron-positron colliding beams for the study of weak interactions," Nucl. Instr. Meth. **136** p47 (1976).

[6] V.I. Telnov, “Restriction on the energy and luminosity of e^+e^- storage rings due to beamstrahlung," Phys. Rev. Lett. **110**, 114801 (2013).

[7] Y. Cai, “Single-particle dynamics in electron storage rings with extremely low emittance", Nucl. Instr. Meth. **A645**, p168 (2011).

[8] K.L. Brown and R.V. Servranckx, “Optics modules for circular accelerator design," Nucl. Instr. Meth., **A258**, p480 (1987).

[9] E. Forest, M. Berz, and J. Irwin, “Normal form methods for complicated periodic systems: a complete solution using differential algebra and Lie operators," Part. Accel. **24** 91 (1989).

[10] K. Oide, “Final focus system with odd-dispersion scheme," KEK Preprint 92-58, July (1992).